DOI: 10.1002/jctb.1191

Biosorption and bioreduction of diamine silver complex by *Corynebacterium*

Haoran Zhang, Qingbiao Li,* Yinghua Lu, Daohua Sun, Xueping Lin, Xu Deng, Ning He and Shuzhen Zheng

Department of Chemical and Biochemical Engineering, Xiamen University, Xiamen 361005, China

Abstract: *Corynebacterium* strain SH09 separated from a silver mine was used for biosorption and bioreduction of diamine silver complex. The biosorption of the diamine silver complex was better than that of silver ions and the maximum of the former was about 350 (mg Ag) (g dried biomass)$^{-1}$. After dried cells of SH09 were resuspended in the aqueous solution of diamine silver complex in the dark at 60 °C for more than 72 h, transmission electron microscopy (TEM) observations showed that a large quantity of black particles whose diameter ranged from 10 to 15 nm were formed on the cell wall. The particles were identified as being silver nanoparticles by X-ray diffraction (XRD) and UV-vis spectroscopy. Under the same conditions, no bioreduction of silver nitrate was found. According to IR spectra, some functional groups, such as the amide of the proteins, were involved in the processes of biosorption and bioreduction.

Keywords: silver nanoparticles; bioreduction; biosorption; diamine silver complex; *Corynebacterium*

1 INTRODUCTION

Biosorption has been shown to be an effective way for the removal and recovery of environmental heavy metals. Studies have shown that the process of biosorption is not simply the adsorption of metal ions onto the microbial biomass and, in some cases, may be accompanied by the reduction of metal ions. Therefore, biosorption coupled to bioreduction is increasingly being recognized as an interesting aspect of the interaction between metal ions and microbes. Many studies have confirmed that enzymatic catalysis and non-enzymatic reduction are two important mechanisms involved in bioreduction. It has been shown that many microorganisms are able to conserve energy through bioreduction of metals, which mostly happens under anaerobic conditions; and in different microorganisms, various enzymes are believed to take an active part in the bioreduction process of transporting electrons from certain electron donors to metal electron acceptors,[1] whilst some studies proved that dried cells of some microorganisms can also reduce some metals such as Au^{3+}.[2] In these cases, no involvement of biological enzymes was observed. Some studies of this non-enzymatic reduction mechanism suggested that some organic functional groups of microbial cell walls could be responsible for the bioreduction process under certain conditions.[3] Studies on the biosorption of Ag^{+} by some microoganisms have been reported,[4,5] and the process of biosorptive accumulation has been well studied.[6] Correspondingly, bioreduction of Ag^{+} has also been investigated. Bioreduction of aqueous Ag^{+} ions by the fungus *Verticillium* AAT-TS-4 or *Fusarium oxysporum* was demonstrated to be a novel method of the synthesis of silver nanoparticles.[7,8] *Pseudomonas stutzeri* AG259 was found to accumulate silver particles at the cell poles and some periplasmic silver-binding enzyme might be involved in this process.[9] Dried biomass of some microorganisms, such as *Lactobacillus* A09, also had the ability to reduce Ag^{+} ions through the interaction between Ag^{+} and some groups on the microbial cell walls.[10] This research is driven both by the need to understand the mechanisms of non-enzymatic bioreduction, which is coupled with biosorption, and also by the possibility of making use of such activity for future biotechnological applications. These include the bioremediation of Ag-contaminated water and silver recovery combined with the formation of novel biocatalysts.

As the reduction of diamine silver complex occurs readily under certain conditions, we studied biosorption and bioreduction of diamine silver complex by a microbe, *Corynebacterium* strain SH09. The formation of silver nanoparticles on the cell wall after bioreduction was further confirmed by means of X-ray diffraction (XRD), transmission electron microscopy (TEM) and UV-vis spectroscopy.

* Correspondence to: Qingbiao Li, Department of Chemical and Biochemical Engineering, Xiamen University, Xiamen 361005, China
E-mail: kelqb@jingxian.xmu.edu.cn
Contract/grant sponsor: National Natural Science Foundation of China; contract/grant number: 20376076
(*Received 20 August 2004; revised version received 23 September 2004; accepted 23 September 2004*)
Published online 13 December 2004

2 MATERIALS AND METHODS

2.1 Bacterial strain

Corynebacterium strain SH09 was isolated from the soil around the sewage outfall of Shanghang silver mine, Fujian, China.

2.2 Culture and collection techniques

Inoculum 1×10^{-3} dm^3 was transferred into 50×10^{-3} dm^3 medium containing final concentrations of 1% (w/v) soya peptone and 0.5% (w/v) beef extract in Erlenmeyer flasks. Cells were grown at 30 °C for 24h and then harvested by centrifugation (3000 r min^{-1}, 10 min at room temperature). The cell pellet was resuspended and centrifuged three times in deionized water.

2.3 Determination of biosorption capacity

Diamine silver complex ($[Ag(NH_3)_2]^+$) solution was prepared by adding ammonia solution ($NH_3 \cdot H_2O$, 25% w/w, AR)into aqueous solution of silver nitrate ($AgNO_3$, AR) until the precipitate of AgOH was transformed into soluble $[Ag(NH_3)_2]^+$. Nitric acid (HNO_3, 65%, AR) and ammonia solution were used to adjust the pH values of silver nitrate and diamine silver complex solutions, respectively. The Ag concentrations of absorbate (silver nitrate or diamine silver complex concentrations in aqueous solutions) were adjusted by controlling the initial additions of silver nitrate into deionized water.

Dried biomass of SH09 cell was resuspended in aqueous solutions of silver nitrate or diamine silver complex at different pH values to obtain a concentration of 5 g of dried biomass per dm^3, and then shaken at a rotation rate of 150 r min^{-1} in the dark at 30 °C. The equilibration time of biosorption was determined by measuring Ag (Ag^+ or $[Ag(NH_3)_2]^+$) solution concentration at intervals, fixing initial $[Ag(NH_3)_2]^+$ concentration at 2000 mg dm^{-3}. After biosorption reached equilibrium, the bacterial cells were separated from suspension by centrifugation (8000 r min^{-1}, 10 min at room temperature), and then assayed for group changes by Fourier transmission infrared spectroscopy (FTIR) (Nicolet Avatar 660; Nicolet, USA). The concentration of Ag in the supernatant was measured by Atomic absorption spectrophotometers (Pgeneral, China). The specific uptake of Ag was then calculated as follows:

$$Q\ (\text{mg g}^{-1}) = V(C_\text{i} - C_\text{r})/M_\text{b}$$

where V was the volume of sample solution (dm^3), C_i and C_r were the initial and residual Ag concentration (mg dm^{-3}) in solution, respectively, and M_b was the dried biomass (g).

2.4 Determination of bioreduction

Dried biomass was resuspended at a concentration of 5 g dm^{-3} in an aqueous solution containing 10 000 mg dm^{-3} Ag^+ or $[Ag(NH_3)_2]^+$ and kept in the dark for different periods of time. Samples of suspension were taken and assayed for the determination of formation of Ag by UNICAM UV-300 spectrophotometers (Thermo Spectronic) at intervals. After bioreduction, the suspension was centrifuged (8000 r min^{-1}, 20 min at room temperature) and the cells were collected for the determination of the formation of Ag, observations of cells and group changes by an X'Pert Pro X-ray Diffractometer (PANalytical BV, The Netherlands), an H-600 Electron Microscope (Hitachi, Japan), a TECNAI F30 FEG TEM (field emission gun, transmission electron microscopy) (Philips, The Netherlands) and FTIR Nicolet Avatar 660 (Nicolet, USA).

3 RESULTS AND DISCUSSION

3.1 Effect of contact time on biosorption

As shown in Fig 1, after 300 min, the specific uptake of $[Ag(NH_3)_2]^+$ was close to its maximum. Thus, 6 h was long enough for the completion of biosorption of $[Ag(NH_3)_2]^+$. Figure 2 shows that the specific

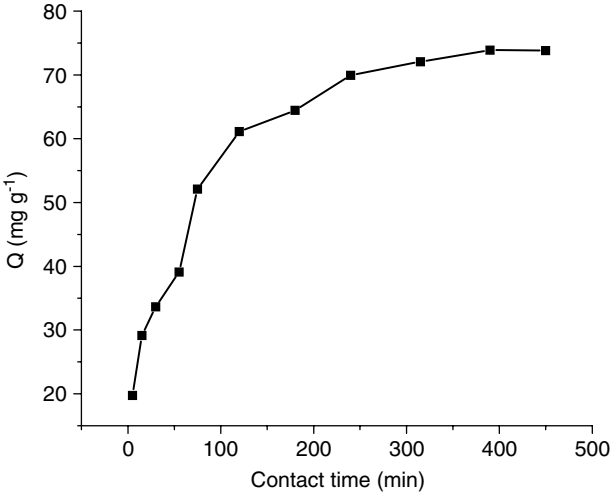

Figure 1. Effect of contact time on the specific uptake of $[Ag(NH_3)_2]^+$ at pH 8 (dried biomass concentration 5 g dm^{-3}, initial Ag concentration 2000 mg dm^{-3}, temperature 30 °C at 150 r min^{-1}).

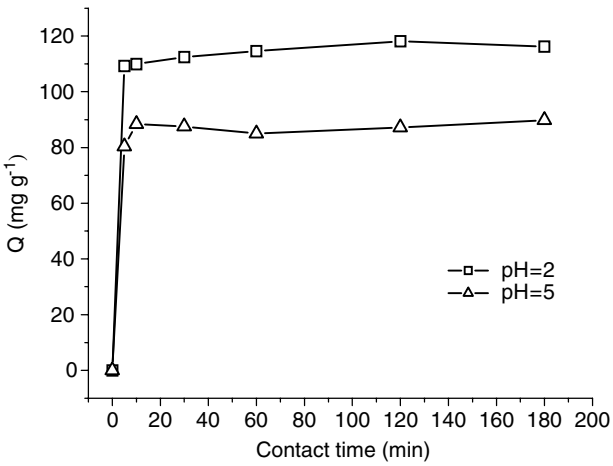

Figure 2. Effect of contact time on the specific uptake of Ag^+ at different pH values (dried biomass concentration 5 g dm^{-3}, initial Ag concentration 2000 mg dm^{-3}, temperature 30 °C at 150 r min^{-1}).

uptake of Ag^+ at pH 2 and 5 did not vary a lot after 5 min, indicating that biosorption of Ag^+ was much quicker than that of $[Ag(NH_3)_2]^+$. This might be because $[Ag(NH_3)_2]^+$ was much larger than Ag^+ and its binding to active biosorption sites could be more difficult due to the effect of steric hindrance; thus biosorption of $[Ag(NH_3)_2]^+$ needed a longer time to reach equilibrium.

3.2 Biosorption of Ag^+ and $[Ag(NH_3)_2]^+$

Figure 3 shows the effect of Ag concentration on biosorption of Ag^+ and $[Ag(NH_3)_2]^+$ at different pH values. The specific uptake of Ag^+ and $[Ag(NH_3)_2]^+$ at different pH values increased with the initial concentration. In the initial Ag concentration range from 250 to 1000 mg dm^{-3}, the specific uptakes of Ag^+ and $[Ag(NH_3)_2]^+$ were almost the same. In the range from 1000 to 6000 mg dm^{-3}, the specific uptake of Ag^+ at pH 2 was the largest. As the initial Ag concentration exceeded 6000 mg dm^{-3}, the specific uptake of $[Ag(NH_3)_2]^+$ at pH 8 was much larger than those of Ag^+. The maximum of the former was above 350 mg g^{-1}.

Throughout the concentration range examined, the biosorption of Ag^+ solution at pH 2 was better than at pH 5, which contrasted with the results of Pethkar and Paknikar.[11] This could be explained as follows: some cell wall constituents of SH09 might be hydrolyzed to a greater degree at the lower pH value, which hindered cell aggregation and partially degraded the bacterial cell wall. More active sites were thus exposed for biosorption. Compared with Ag^+, $[Ag(NH_3)_2]^+$ was subject to greater steric hindrance in the process of biosorption. However, the specific uptake of $[Ag(NH_3)_2]^+$ was higher than that of Ag^+. As both of the moieties are positively charged, ion exchange and adsorption could not make such a difference. Therefore, the reasons for the high uptake of $[Ag(NH_3)_2]^+$ might include: (1) effect of competing H^+ was reduced in basic surroundings; (2)more negatively-charged groups were formed in basic solution, which adsorbed more $[Ag(NH_3)_2]^+$ through electrostatic interaction; (3) $[Ag(NH_3)_2]^+$ had a high affinity to the functional groups of the cell wall.

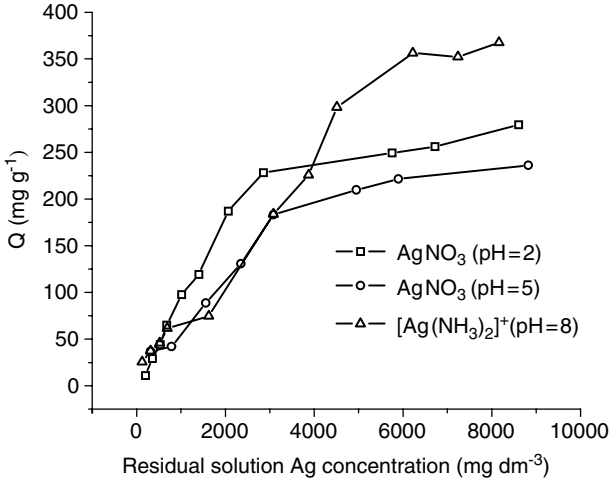

Figure 3. Effect of Ag concentration on biosorption by *Corynebacterium* SH09 (dried biomass concentration 5 g dm^{-3}, temperature 30 °C, contact time 6 h at 150 r min^{-1}).

3.2 Bioreduction of $[Ag(NH_3)_2]^+$

3.2.1 Effect of bioreduction time

UV–vis absorption spectra have been proved to be useful in indicating the formation of silver particles. The absorption peak at about 400 nm is the characteristic surface plasmon absorption peak of silver nanoparticles and the position of the absorption peak depends on the particles size and shape.[12,13]

Temperature greatly influenced bioreduction, as shown by the earlier appearance of the characteristic Ag(0) band at higher temperature. In the temperature range of our study (20–60 °C), 60 °C was the most favorable for bioreduction. Figure 4 presents the absorption spectra of silver nanoparticles formed through the process of the bioreduction of $[Ag(NH_3)_2]^+$ by SH09 at 60 °C.

After 36 h, an obvious characteristic plasmon absorption maximum at 430 nm became evident, indicating the formation of silver nanoparticles. The intensity of the absorption peak increased with time and reflected increased formation of silver particles. After 96 h, the characteristic absorption peak was centered at 440 nm, shifting towards longer wavelengths for about 10 nm, which suggested the increasing size of silver particles. Previous study has shown that the size of silver nanoparticles prepared by chemical reduction increased with time, which is in good agreement with our result.[14] No characteristic plasmon absorption peak was found in the same time range in the case of Ag^+. This result is similar to the finding of Esumi *et al*[15] that in acid solution, no reduction of Ag^+ ions took place in the presence of sugar-persubstituted poly(amidoamine) dendrimers, which may be due to the lack of favorable thermodynamic conditions for the reduction of Ag^+.

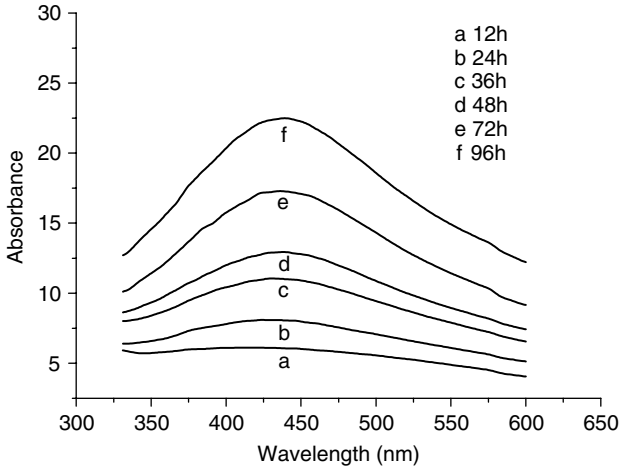

Figure 4. Absorption spectra of silver nanoparticles after bioreduction by *Corynebacterium* strain SH09 at 60 °C. The initial concentration of $[Ag(NH_3)_2]^+$ and dried biomass were 10 000 mg dm^{-3} and 5 g dm^{-3}, respectively.

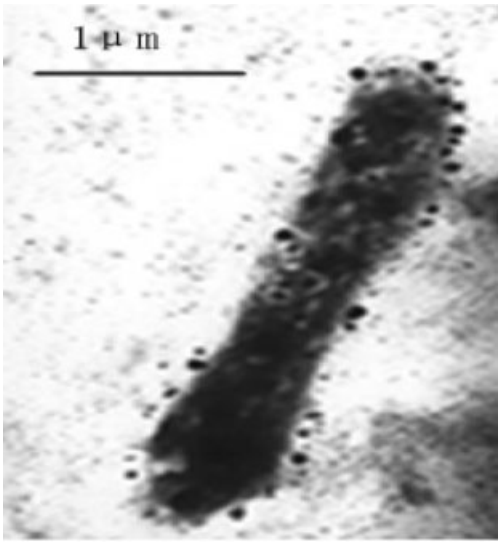

(a)

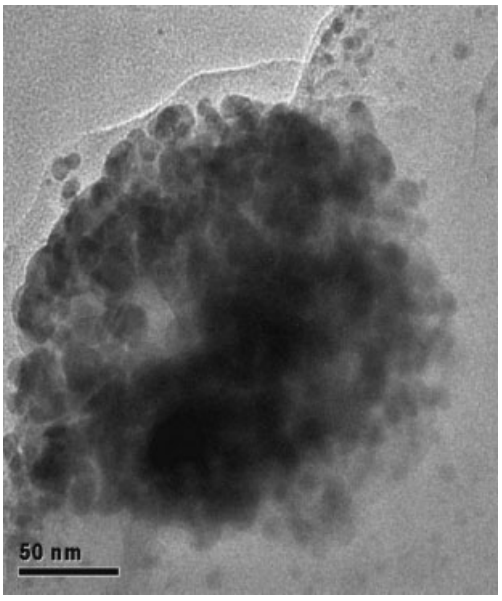

(b)

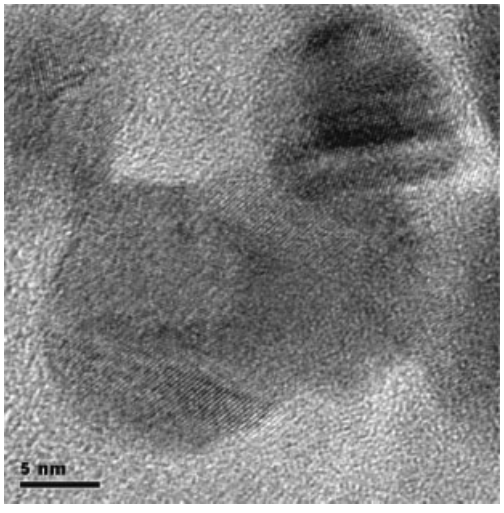

(c)

Figure 5. Transmission electron micrographs of nanoparticles after bioreduction of $[Ag(NH_3)_2]^+$ at 60 °C. The initial Ag and dried biomass concentrations were 10 000 mg dm^{-3} and 5 g dm^{-3}, respectively. Contact time was 72 h.

3.2.2 Observation of silver nanoparticles

Transmission electron micrographs shown in Fig 5(a) display the cell of SH09 after 72 h of bioreduction at 60 °C. A great quantity of black particles on the cell wall can be observed, whose diameters are below 100 nm. Higher-magnification images of these particles (Fig 5(b)) further indicate that they are in fact composed of many smaller separate particles. Fig 5(c) shows their diameter ranges from 10 to 15 nm. The particles, on the cell wall were identified as containing a great deal of Ag using energy dispersive x-ray spectrometry (Fig 6) and confirmed as elemental Ag(0) using XRD (Fig 7). The calculation of the crystal size from the XRD data showed that the average diameter of Ag(0) crystals accumulated on the cell wall was about 9.9 nm, close to the results obtained from TEM. No characteristic peak of elemental Ag(0) was found in the XRD pattern under the same conditions when Ag^+ was used. Likewise, the control sample, containing only $[Ag(NH_3)_2]^+$ without the addition of SH09 biomass, did not cause the appearance of these peaks in the XRD pattern.

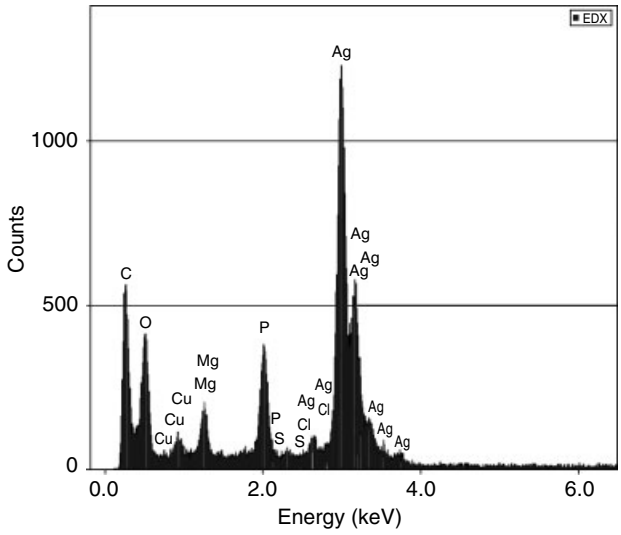

Figure 6. Energy-dispersive X-ray spectrum of nanoparticles on the cell wall. The different X-ray emission peaks are labeled.

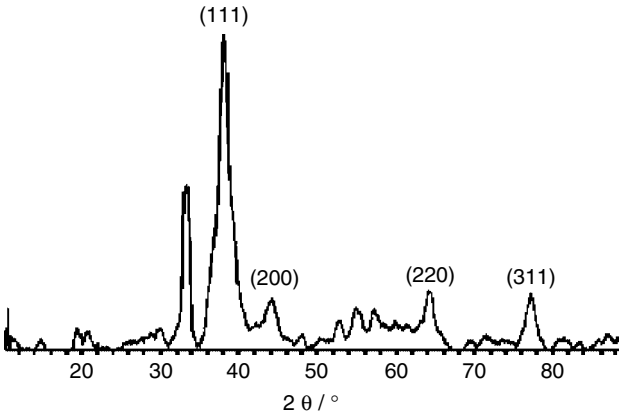

Figure 7. X-ray diffraction pattern of silver nanoparticles on the cell wall (smoothed). Labeled peaks correspond to the characteristic diffraction peaks of elemental Ag(0).

The formation of silver nanoparticles on the cell walls of *Corynebacterium* strain SH09 may be explained as follows. As suggested by previous studies, the biosorption and bioreduction of silver ions could occur on the cell wall;[7,16] it is possible to hypothesize that $[Ag(NH_3)_2]^+$ was first trapped on the cell wall through biosorption. Thereafter, some groups on the cell wall reduced $[Ag(NH_3)_2]^+$ and bound the formed Ag(0) nuclei onto the cell wall, which further grew into Ag(0) clusters or crystals. The aggregation effect between these crystals might be reduced due to their strong interaction with the groups of the cell wall. Consequently, instead of individual crystals increasing in size, these crystals only formed bigger aggregates composed of separate Ag(0) crystals.

3.2.3 Group changes on cell wall via biosorption and bioreduction

FTIR absorption spectra of biomass of *Corynebacterium* strain SH09 before and after biosorption and bioreduction (Fig 8) can yield information regarding the chemical change of the functional groups involved in biosorption and bioreduction. As *Corynebacterium* SH09 is Gram-positive, the D-Glu-containing tetrapeptide in peptidoglycan is prevalent in the cell wall. Thereafter, the absorbance band at 1658 cm^{-1} in Curve (a) was associated with the carbonyl stretch vibration in the amide linkages of peptide chains. The band at 1541 cm^{-1} was identified as another amide band, which arose due to the combination of N–H bending mode and C–N stretch vibration mode. The ionized carboxyl of some amino acid residues, such as D-Glu residues, caused the appearance of two bands: the first band at around 1650 cm^{-1} was attributed to symmetrical stretch vibration of COO^- and overlapped with the band of carbonyl stretch vibration in amide linkages; the second band at 1392 cm^{-1} was attributed to asymmetrical stretch vibration of COO^-.

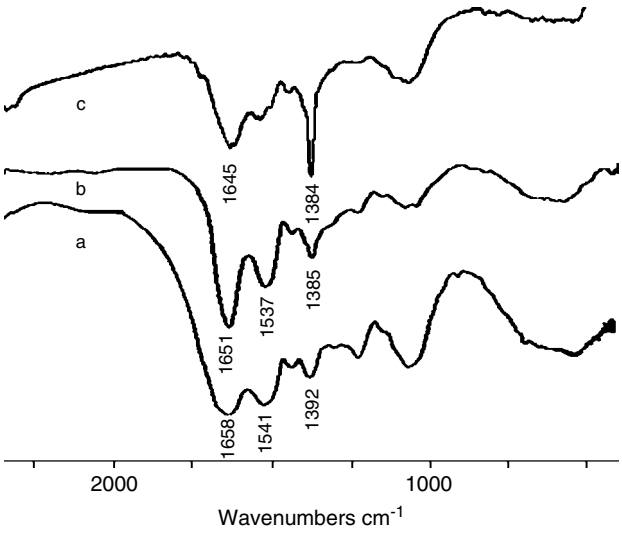

Figure 8. FTIR absorption spectra of *Corynebacterium* strain SH09 biomass before biosorption (a), after biosorption (b) and after bioreduction (c).

After biosorption, the three bands shifted to 1651 cm^{-1}, 1537 cm^{-1} and 1385 cm^{-1}, respectively, which indicated that amide, specifically C=O and C–N, and ionized carboxyl were involved in the process of biosorption.

After bioreduction, the band at 1657 cm^{-1} shifted to 1645 cm^{-1}, the intensity of band at 1541 cm^{-1} decreased, and the band at 1392 cm^{-1} moved to 1384 cm^{-1}, showing that both amide and ionized carbonyl had been combined with $[Ag(NH_3)_2]^+$ or Ag(0) through bioreduction. The increase in the intensity of the band at 1384 cm^{-1} in Curve(c) suggested that some reducing groups such as aldehyde and ketone of the cell wall might be oxidized to carboxyl and then combined with $[Ag(NH_3)_2]^+$ or Ag(0) through bioreduction, intensifying the band at 1384 cm^{-1}.

4 CONCLUSION

Corynebacterium strain SH09 had strong biosorption ability for $[Ag(NH_3)_2]^+$ and the maximum specific uptake could be above 350 (mg Ag) (g dried biomass)$^{-1}$. Under certain conditions, SH09 could also reduce $[Ag(NH_3)_2]^+$ to elemental Ag(0). The ionized carboxyl of amino acid residues and the amide of peptide chains were the main groups trapping $[Ag(NH_3)_2]^+$ onto the cell wall and some reducing groups, such as aldehyde and ketone, were involved in subsequent bioreduction. Since the combination with the functional groups of the cell wall of SH09 might reduce the aggregation effect of the formed Ag(0) crystals, the average size of silver particles was kept around 10–15 nm, which suggested the potential use of this study in the industrial synthesis of silver nanoparticles.

ACKNOWLEDGEMENTS

This work is part of the project (20376076) supported by National Natural Science Foundation of China. The authors thank the Analysis and Testing Center of Xiamen University for the analysis and measurement work in this study.

REFERENCES

1 Lloyd JR, Microbial reduction of metals and radionuclides. *FEMS Microbiol Rev* **27**:411–425 (2003).
2 Liu YY, Fu JK, Chen P, Yu XS and Yang PC, Studies on biosorption of Au^{3+} by *Bacillus megaterium*. *Acta Microbiologica Sinica* **40**:425–429 (2000).
3 Lin ZY, Fu JK, Wu JM, Liu YY and Cheng Hu, Preliminary study on the mechanism of non-enzymatic bioreduction of precious metal ions. *Acta Phys-Chim Sin* **17**:477–480 (2001).
4 Pethkar AV, Kulkarni SK and Paknikar KM, Comparative studies on metal biosorption by two strains of *Cladosporium cladosporioides*. *Bioresource Technol* **80**:211–215 (2001).
5 Gomes NCM, Rosa CA, Pimentel PF and Mendonca-Hagler LCS, Uptake of free and complexed silver ions by different strains of *Rhodotorula mucilaginosa*. *Braz J Microbiol* **33**:62–66 (2002).

6 Tsezos E, Remoudaki E and Angelatou V, A systematic study on equilibrium and kinetics of biosorptive accumulation. The case of Ag and Ni. *Int Biodeter Biodegr* **35**:129–153 (1995).
7 Mukherjee P, Ahmad A, Mandal D, Senapati S, Sainkar SR, Khan MI, Parishcha R, Ajaykumar PV, Alam M, Kumar R and Sastry M, Fungus-mediated synthesis of silver nanoparticles and their immobilization in the mycelial matrix: a novel biological approach to nanoparticle synthesis. *Nano Lett* **1**:515–519 (2001).
8 Ahmad A, Mukherjee P, Senapati S, Mandal D, Khan MI, Kumar R and Sastry M, Extracellular biosynthesis of silver nanoparticles using the fungus *Fusarium oxysporum*. *Colloid Surf B-Biointerf* **28**:313–318 (2003).
9 Klaus T, Joerger R, Olsson E and Granqvist CG, Silver-based crystalline nanoparticles, microbially fabricated. *Proc Natl Acad Sci USA* **96**:13 611–13 614 (1999).
10 Fu JK, Liu YY, Gu PY, Tang DL, Lin ZY, Yao BX and Weng SZ, Spectroscopic characterization on the biosorption and bioreduction of Ag(I) by *Lactobacillus* sp A09. *Acta Phys-Chim Sin* **16**:779–782 (2000).
11 Pethkar AV and Paknikar KM, Thiosulfate biodegradation–silver biosorption process for the treatment of photofilm processing wastewater. *Process Biochem* **38**:855–860 (2003).
12 Kapoor S, Preparation, characterization, and surface modification of silver particles. *Langmuir* **14**:1021–1025 (1998).
13 Zhu JJ, Liu SW, Palchik O, Koltypin Y and Gedanken A, Shape-controlled synthesis of silver nanoparticles by pulse sonoelectrochemical methods. *Langmuir* **16**:6396–6399 (2000).
14 Lee MH, Oh SG, Suh KD, Kim DG and Sohn D, Preparation of silver nanoparticles in hexagonal phase formed by nonionic Triton X-100 surfactant. *Colloid Surf A-Physciochem Eng Asp* **210**:49–60 (2002).
15 Esumi K, Hosoya T and Suzuki A, Formation of gold and silver nanoparticles in aqueous solution of sugar-persubstituted poly(amidoamine) dendrimers. *J Colloid Interf Sci* **226**:346–352 (2000).
16 Tsezos M, Remoudaki E and Angelatou V, Biosorption sites of selected metals using electron microscopy. *Comp Biochem Physiol A-Physiol* **118**:481–487 (1997).